International Journal of Biological Macromolecules 74 (2015) 458–466

Contents lists available at ScienceDirect

International Journal of Biological Macromolecules

journal homepage: www.elsevier.com/locate/ijbiomac

Adsorption of chromium from aqueous solutions using crosslinked chitosan–diethylenetriaminepentaacetic acid

Ronak Bhatt[a], B. Sreedhar[b], P. Padmaja[a,*]

[a] Department of Chemistry, Faculty of Science, The M. S. University of Baroda, Vadodara 390002, India
[b] Inorganic and Physical Chemistry Division, Indian Institute of Chemical Technology, Hyderabad 500007, India

ARTICLE INFO

Article history:
Received 24 October 2014
Received in revised form
16 December 2014
Accepted 23 December 2014
Available online 3 January 2015

Keywords:
Adsorption
Chitosan
Diethylenetriaminepentaacetic acid
Chrome-plating effluent

ABSTRACT

Chitosan (CH) and its derivatives have been the focus of attention for researchers as potential adsorbents for heavy metal removal. The adsorption potential of chitosan cross-linked with diethylenetriaminepentaacetic acid (CD) for Cr^{6+} was investigated. CD was characterized by FTIR, XRD, TGA, XPS and ESR techniques. Batch experiments were conducted to optimize the parameters affecting the adsorption of chromium. The optimum pH was found to be 3 and the adsorption process was found to be exothermic. Adsorption isotherms were determined and the maximum adsorption capacity of CD for chromium was found to be 192.3 mg/g which was higher than the adsorption capacity of the adsorbents reported in literature. The thermodynamic parameters, such as Gibbs free energy, changes in enthalpy and changes in entropy change were also evaluated. XPS and ESR studies revealed that Cr^{6+} adsorbed onto CD was reduced to Cr^{3+}. The efficacy of CD for removal of Cr^{6+} from chrome plating effluent was demonstrated.
© 2015 Elsevier B.V. All rights reserved.

1. Introduction

Chromium is one of the major contaminants in wastewater as it is widely used in industries, the most important sources being pigments, electroplating, leather and mining industries. Chromium is present in the aqueous environment as Cr^{3+} and Cr^{6+}. Hexavalent chromium exists in water as oxyanions such as chromate ($HCrO_4^-$) and dichromate ($Cr_2O_7^{2-}$) [1]. While Cr^{3+} is essential to human metabolism at low concentrations, Cr^{6+} is toxic and carcinogenic [2]. Due to its severe toxicity, US EPA and ISS India IS:10500 set the tolerance limit for the discharge of Cr^{6+} ions into surface water as 0.1 mg/L and in potable water as 0.05 mg/L [3,4].

Cr^{6+} is mainly removed from wastewaters by its reduction to Cr^{3+} with the use of various chemical reductants and microorganisms which require the use of expensive and toxic chemical reductants/nutrients [5,6]. Furthermore, cell death also occurs due to the toxicity of Cr^{6+}. Bio-adsorption using agro-waste/biomass and biopolymers has been adopted as an effective method to remove chromium and other toxic metals from aqueous environments [7–9]. During the past three decades, the use of CH as a bio-adsorbent has been gaining increased attention [10]. The adsorption and chelating properties of chitosan were further improved by functionalization or derivatization [11]. For instance, CH has been modified by different ligands such as barbituric acid, oxine, glycine, iminodiaceticacid (IDA), ethyleneglycol-bis(2-aminoethylether)-*N*,*N*,*N*′,*N*′-tetraacetic acid (EGTA), ethylenediaminetetraacetic acid (EDTA) and diethylenetriaminepentaacetic acid (DTPA) [5,12–19]. Evelina Repo et al. have used EDTA-modified CH for the removal of Co(II) in the presence of EDTA and other interfering species from aqueous solutions [20]. They also had modified CH-silica hybrid with EDTA and used them as adsorbent for the removal of cobalt, nickel, cadmium and lead ions from aqueous solutions [21]. They further have reviewed the use of amino polycarboxylic acid functionalized adsorbents for the removal of heavy metals from water [22]. Chitosan grafted with poly(ethylene imine) and cross-linked with epichlorohydrin has been used by Kyzas et al. for the simultaneous removal of a reactive dye and Cr^{6+} [23]. They also had investigated the potential of *N*-(2-carboxybenzyl)-grafted CH for the removal of both positively charged (Cu(II), Ni(II)) and negatively charged (Cr(VI), As(V)) metal ions from aqueous solutions as well as succinyl grafted chitosan for the removal of zinc and cationic dye from binary mixtures [24,25]. Zarebsiki first used DTPA for the determination of trace levels of Cr^{3+} using several polarographic techniques [26]. This method has been improved using a hanging mercury drop electrode (HMDE) for the speciation analysis of chromium in different media. The complexation of Cr^{3+} and Cr^{6+} with diethylenetriaminepentaacetic acid (DTPA), the redox behavior of these complexes and their adsorption

* Corresponding author. Tel.: +91 265 2795552/9376214733; fax: +91 265 2795552.
E-mail addresses: ppadmaja2010@yahoo.in, p_padmaja2001@yahoo.com (P. Padmaja).

http://dx.doi.org/10.1016/j.ijbiomac.2014.12.041
0141-8130/© 2015 Elsevier B.V. All rights reserved.

on the mercury electrode surface were investigated by Sander et al. using electrochemical techniques and UV–vis spectroscopy [27].

DTPA-modified chitosan as well as silica gel have been used by Evelina Repo et al. for the removal of cobalt as its EDTA complex [28]. However, the adsorption potential of CD for chromium has not been studied earlier. Bearing these factors in mind it was felt that chemical modification of CH with diethylentriaminepentaacetic acid (DTPA) may result in an adsorbent for chromium with interesting binding properties. Our objective was thus to synthesize chitosan DTPA complex and study its potential for adsorption of Cr^{6+} as well its reduction to Cr^{3+}. The potential of CD in the treatment of chrome plating effluent with minimum manipulation in original pH of the effluent has also been investigated.

2. Materials and Methods

2.1. Materials

All the reagents used were of AR grade. CH from Crab shells (Sigma Aldrich, USA) and DTPA (National Chemicals, India) were used as such without further grinding and sieving.

2.2. Synthesis of adsorbents (chitosan crosslinked with DTPA)

A 100 ml of 1% CH in 1% acetic acid solution was added to 100 ml of 0.5 M solution of DTPA (DTPA dissolved in 0.41 M NaOH) and stirred for 24 h for the formation of cross-linked CH with DTPA (CD). A white gel material was formed which was then filtered, washed with double distilled water to neutral and dried overnight in vacuum oven at 30 °C. The material was then crushed well and sieved with mesh size of 180 microns for obtaining uniform size of adsorbent.

2.3. Preparation of metal solutions

Stock solution of 1000 ppm Cr^{6+} was prepared by dissolving 5.6653 g of potassium dichromate (99.92% assay) in 1 L of double-distilled water. Working standards were prepared by diluting different volumes of the stock solution to obtain the desired concentration.

2.4. Batch adsorption experiments

Batch adsorption experiments were conducted at 30 °C by agitating 0.05 g adsorbent with 25 ml of Cr^{6+} solution of desired concentration at optimum pH (pH 3) in 100 ml of stoppered conical flask in thermostated rotary mechanical shaker at 200 rpm for 4 h at 30 °C except for pH optimization experiments. The pH range at which the maximum chromium uptake occurred was determined by varying the initial pH of the solution in the range 1–11 using H_2SO_4 and NaOH. The optimum equilibrium time was determined by varying the contact time in the range of 60–240 min. In each experiment, after agitation the contents of the flasks were filtered. The Cr^{6+} concentration in the filtrate was subsequently determined colorimetrically at 540 nm by UV Spectrophotometer (Jasco V630 model) after complexation with 1,5-diphenylcarbazide [29]. The uptake of Cr^{6+} was calculated according to Eq. (1).

$$Q_e = \frac{C_i - C_e}{m} \quad (1)$$

where Q_e represents the amount of Cr^{6+} adsorbed per gram of adsorbent and m represents the mass of adsorbent in g/L. C_i and C_e (ppm) are the initial and equilibrium (after adsorption) concentrations of Cr^{6+} in solution, respectively. In order to ensure the reproducibility of results, experiments were replicated three times and data presented were the mean values from these independent experiments.

Table 1
Isotherm model constants for Cr^{6+}-loaded CD.

Freundlich		*Langmuir*	
K_f (L g^{-1})	5.7524	K_L (L mmol^{-1})	0.0098
N	1.8423	q_m (mg/g)	192.31
r^2	0.9889	r^2	0.983
Temkin-1		*Halsey*	
K_T (L mmol^{-1})	0.1352	k_H (L g^{-1})	4.4042
r^2	0.9984	n_H	−1.5694
		r^2	0.9918
Elovich		*F-H Isotherm*	
q_m (mg/g)	77.4593	Nfh	−3.2584
K_E (L mmol^{-1})	0.0294	r^2	0.9955
r^2	0.9977	Kfh	0.0001
Lnqm	4.3497		

Adsorption isotherms were determined by the treatment of 0.05 g of CD with 50 ppm Cr^{6+} in a rotary mechanical shaker. After agitation, the contents of the flasks were filtered. The concentration of Cr^{6+} remaining in the solution was determined. The experiments were replicated three times and data presented were the mean values from these independent experiments. The results of experimental measurements were plotted in the form of adsorption isotherms and the standard deviations for the replicate measurements were expressed as error bars in Figs. S1 and S2. Attempts were made to fit the equilibrium metal sorption isotherm data to a number of well-known models (Table S1 [44–49]) like linear forms of Freundlich, Langmuir, Temkin, Flory–Huggins and Halsey to gain insights into the processes governing adsorption. The results are shown in Table 1.

The efficiency of the adsorption process was also assessed by treating the kinetic sorption data of Cr^{6+} onto CD with pseudo-first-order, pseudo-second-order, intraparticle diffusion, Bangham and Liquid film diffusion models (Table S2 [50–55]). The values of correlation coefficients and standard deviation were used to compare the models which are shown in Table 2.

The thermodynamic parameters of the adsorption process could be determined from the experimental data obtained at various temperatures using Eqs. (2)–(4):

$$K_d = \frac{q_e}{c_e} \quad (2)$$

$$\ln K_d = \frac{\Delta S^\circ}{R} - \frac{\Delta H^\circ}{RT} \quad (3)$$

$$\Delta G^\circ = \Delta H^\circ - T\Delta S^\circ \quad (4)$$

Table 2
Kinetic parameters for Cr^{6+}-loaded CD.

Pseudo-second-order		*Lagergren*	
Type1		q_t (mg/g)	5.6798
Experimental q_t (mg/g)	20.631	K	0.0147
q_t (mg/g)	21.5331	r^2	0.9972
K	0.0042	*Intraparticle*	
r^2	0.9999	K	0.2956
Type2		r^2	0.9741
q_t (mg/g)	21.3903	*Elovich*	
K	0.0046	B	0.6031
r^2	0.9919	A	1817.8
Type3		r^2	0.9962
q_t (mg/g)	21.4007	*Liquid film diffusion model*	
K	0.0046	K_{FD}	0.0147
r^2	0.9898	r^2	0.9973
Type4		*Bangham*	
q_t (mg/g)	21.4172	Km	−34.2082
K	0.0045	A	0.1998
r^2	0.9897	r^2	0.9992

Table 3
Thermodynamic parameters for adsorption of Cr^{6+} onto CD.

Temperature (°K)	ΔG kcal/mole
303	−2.1637
313	−0.7683
323	0.6271
333	2.0225
343	3.418
ΔH (kcal/mol)	−44.445
ΔS (cal/mol °K)	−139.542

where K_d is the distribution coefficient. The values of ΔH° and ΔS° can be calculated from the slope and intercept of the plots of $\ln K_d$ against $1/T$ and are shown in Table 3.

2.5. Characterization techniques

FTIR spectra of the samples in the form of KBr pellets were collected with 8 cm^{-1} resolution using a Perkin Elmer RX1 model in the wave number range 400–4000 cm^{-1} by accumulating 16 scans. The surface morphology of CD before and after adsorption of Cr^{6+} was studied with JSM 5610 LV scanning electron microscope. Elemental spectra were obtained using an energy-dispersive X-ray analyzer (EDS) which allowed qualitative detection and localization of elements present in CD before and after Cr^{6+} adsorption. XRD analysis of CD before and after Cr^{6+} adsorption was done using PANalytical'sX'PertPRO XRD instrument in the 2θ range 0–100 using nickel-filtered Cu Kα radiation. EPR spectra were recorded at room temperature using a JES-FA200 ESR JEOL Spectrometer operated in the X-band operating at ~9.65 GHz with a field modulation frequency of 100.00 kHz. Thermogravimetric analysis (TGA) was done using EXSTAR6000 TG/DTA6300-l instrument. The measurements were carried out under a nitrogen atmosphere using a heating rate of 10 °C per minute temperature in the temperature range 30–500 °C. The DSC thermograms were recorded by heating 1.9 mg CH and 2.2 mg CD of samples in the temperature range 30–500 °C with a ramp of 10 °C per minute in a nitrogen stream of 50 ml/min using 822EN Mettler Toledo Model instrument. The KRATOS AXIS Ultra HSA was used for XPS analysis, the de-convolution process of C 1s spectra as well as the elemental composition evaluation may result in an error of up to 5%. All spectra are presented charge balanced and energy referenced to C 1s at 284.6 eV. Chemical states of O, N and C species were determined from the charge corrected hi-resolution scans. The atomic concentrations were estimated based on comparisons of integrated peak intensities normalized by the atomic sensitivity factors.

2.6. Desorption

For desorption studies, 0.05 g of CD preloaded with Cr^{6+} was equilibrated with 25 ml solutions of 0.1 M of NaOH, H_2SO_4, HCl and HNO_3 for 120 min. The contents of the flasks were filtered and the chromium content in the filtrate was determined by ICP. Three consecutive adsorption–desorption cycles were carried out to test the reusability of CD.

2.7. Application to chrome plating effluent

The efficiency of CD to remove chromium from an effluent from a chrome plating industry of GIDC, Ankleshwar, India, was examined. The sample from chrome plating effluent contained not only chromium, but also other metals. 1 M HNO_3 was used to adjust the pH of the effluent to 3 and the concentration of metals after adsorption using 0.05 g CD was determined through ICP.

3. Results and Discussion

3.1. Characterization of CD

3.1.1. IR spectra analysis

The FT-IR spectrum (Fig. 1) of CH showed characteristic bands corresponding to O—H and N—H stretching vibrations at 3619 and 3420 cm^{-1}, respectively. The C—H and the C—O stretching vibrations were obtained at 2857 and 1051 cm^{-1}, respectively. The N—H bending vibration at 1650 cm^{-1} is shifted to 1653 cm^{-1} after grafting with DTPA. Similarly, the C—N bending vibration observed at 1393 cm^{-1} resulted in a shift to 1398 cm^{-1}. These changes could be attributed to the effective grafting of DTPA onto chitosan. The FT-IR spectrum of CD showed bands at 1699, 1398 and 1145 cm^{-1} due to C=O, C—O and C—N stretching, respectively. It is observed that the 1557 cm^{-1} band due to N—H bending vibration of amide II shifted to 1541 cm^{-1} indicating the formation of imide bond in CD. The IR spectrum of metal-loaded adsorbent is also shown in Fig. 1. Cr^{6+} exists mainly as hydrogen chromate ($HCrO_4^-$) and dichromate ($Cr_2O_7^{2-}$) species in acidic medium. Characteristic peaks due to Cr=O and Cr—O were observed in the IR spectrum at 875 and 671 cm^{-1}, respectively.

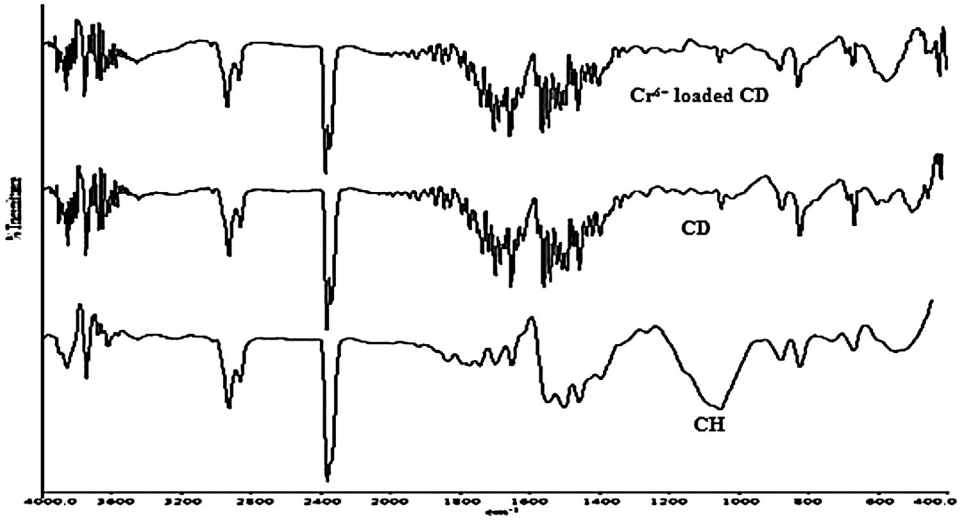

Fig. 1. FTIR spectra of CH, CD and Cr^{6+}-loaded CD.

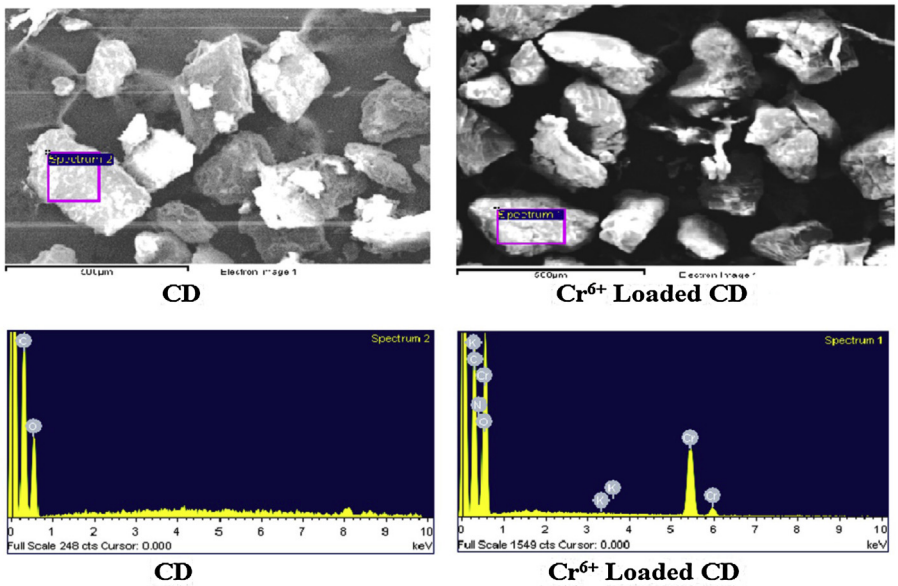

Fig. 2. (a) SEM and (b) EDAX of CD and Cr^{6+}-loaded CD.

3.1.2. SEM and EDAX analysis

Fig. 2a and b shows the SEM and EDAX images of CD and Cr^{6+}-loaded CD. CD did not look porous suggesting that the adsorption properties could be mainly attributed to the functional groups on its surface.

3.1.3. XRD

The X-ray diffraction spectra of CD (Fig. 3) show crystalline areas $2\theta = 10°$, 20°, 26° and 73° (due to grafting of DTPA at the CH backbone), while no such peaks are visible in the XRD of pristine CH. It is observed that the adsorbent has become amorphous after adsorption of chromium with a broad peak at 34.5° confirming the presence of chromium [30,31].

3.1.4. ESR

ESR spectra of CD and Cr^{6+}-loaded CD are shown in Fig. 4. ESR spectra of Cr^{6+}-loaded adsorbent showed a signal with g value of 1.9839 which could be attributed to the exchange coupling between Cr^{3+}–Cr^{3+} ion pairs or large clusters of Cr^{3+} suggesting that adsorption of Cr^{6+} onto CD has resulted in its reduction to Cr^{3+} [32]. Reduction of Cr^{6+} to Cr^{3+} was also reported by Nakajima and Baba [33] on the surface of persimmon tannin gel and Araujo et al. [34] on termite's nest.

3.1.5. TGA and DSC

TGA curves of CH and CD are shown in Fig. 5a. It is seen that there are two weight loss steps in CH and CD. The first one occurred at around 100 °C corresponding to 5 and 8% loss, respectively, for CH and CD which can be attributed to the loss of adsorbed and bound water. This was followed by another weight loss starting at ~240 °C for CH and ~255 °C for CD which can be attributed to deacetylation of chitosan in CH and both degradation of DTPA and deacetylation in CD.

The DSC curve in Fig. 5b of CD shows two peaks: an endothermic peak at 77.18 °C and an exothermic peak at 302.8 °C which could be attributed to evaporation of water from the polymer and oxidative degradation as well as deacetylation [35]. The glass transition temperature of CD was observed to be at 301 °C while for CH it was observed at 306 °C. It was observed that there was a small increase in the decomposition temperature of CD as compared to chitosan.

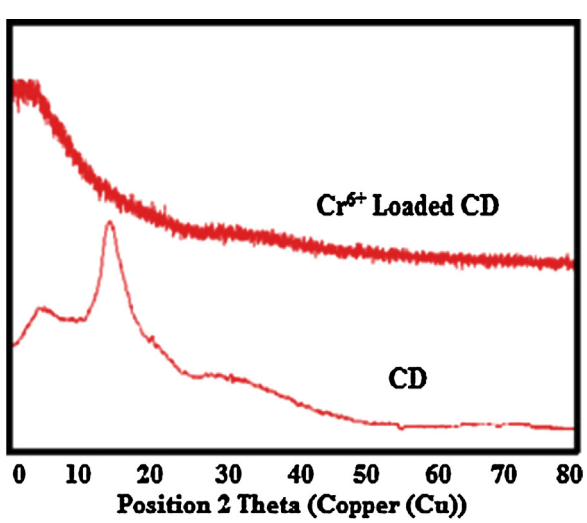

Fig. 3. XRD spectra of CD and Cr^{+6}-loaded CD.

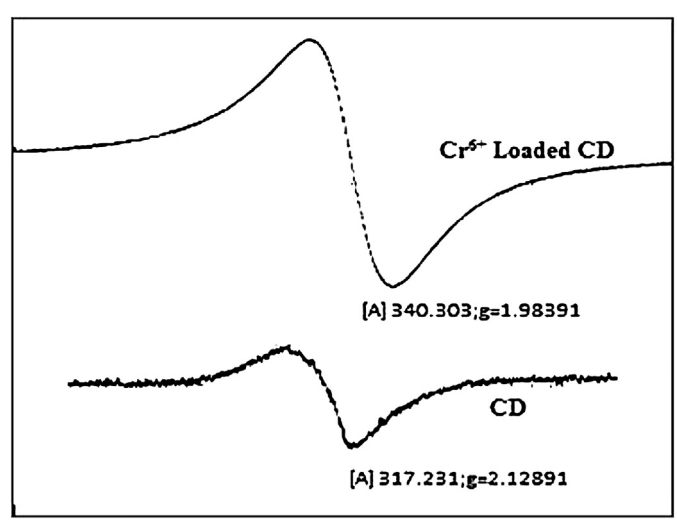

Fig. 4. ESR spectra of CD and Cr^{+6}-loaded CD.

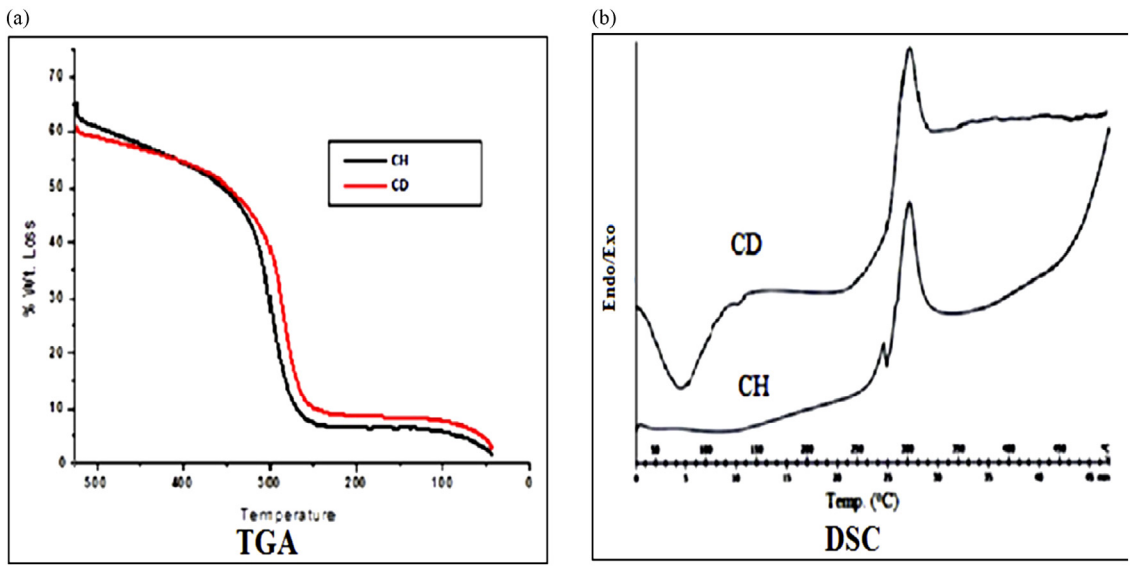

Fig. 5. (a) TGA and (b) DSC of CH and CD.

This could be due to cross-linking of chitosan through DTPA leading to enhanced thermal stability.

3.1.6. XPS

Fig. 6 and Table 4 summarize the binding energies and percentage atomic concentration of CH, CD and chromium-loaded CD. It is observed that the deconvoluted C 1s spectrum of CH and CD comprised of two peaks with BEs ~284.6 and 287.7 eV. These peaks can be assigned to C—C, and O—C—O bonds of alcoholic and ether groups. The carbon atoms of these respective organic functional groups of the adsorbents have different electron densities. Results indicate that the atomic concentration (%) of C—C groups (286.3 eV) increases after complexation with DTPA due to addition of alkyl groups induced by DTPA. However, in CD loaded with chromium there is an additional peak at binding energy 288.1 eV which can be attributed to carbonyl groups bound with chromium.

Table 4
Binding energies of CH, CD and Cr^{6+} loaded CD.

		Binding energy (eV)	FWHM (eV)	%
CH	C 1s	284.6	2.786	81.5
	C 1s	287.0	2.833	18.5
	O 1S	532.2	2.778	100
	N 1S	398.7	2.478	67
	N 1S	400.6	2.81	33
CD	C 1s	284.5	2.521	73
	C 1s	286.5	2.788	27
	O 1S	532.2	2.709	100
	N 1s	398.7	2.654	70.6
	N 1s	400.8	3.175	29.4
Cr^{6+}-loaded CD	C 1S	284.5	2.062	60.6
	C 1S	286.2	2.154	30.7
	C 1S	288.1	1.957	8.7
	O 1S	531.8	3.167	65.8
	O 1S	533.1	2.832	34.2
	N 1S	398.6	1.781	34.3
	N 1S	400.1	1.813	50.6
	N 1S	401.6	1.652	15.1
	Cr 2p	576.9	2.477	38.7
	Cr 2p	585.9	3.765	25.5
	Cr 2p	579.0	2.23	20.2
	Cr 2p	588.5	2.62	15.6

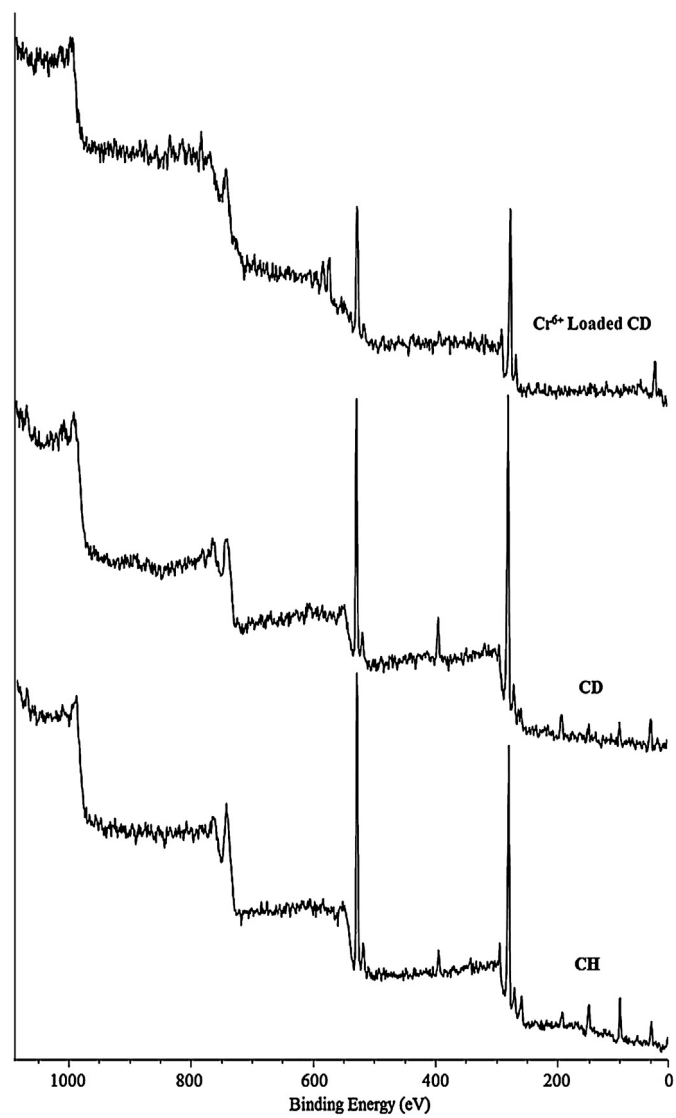

Fig. 6. XPS spectra of CH, CD and Cr^{+6}-loaded CD.

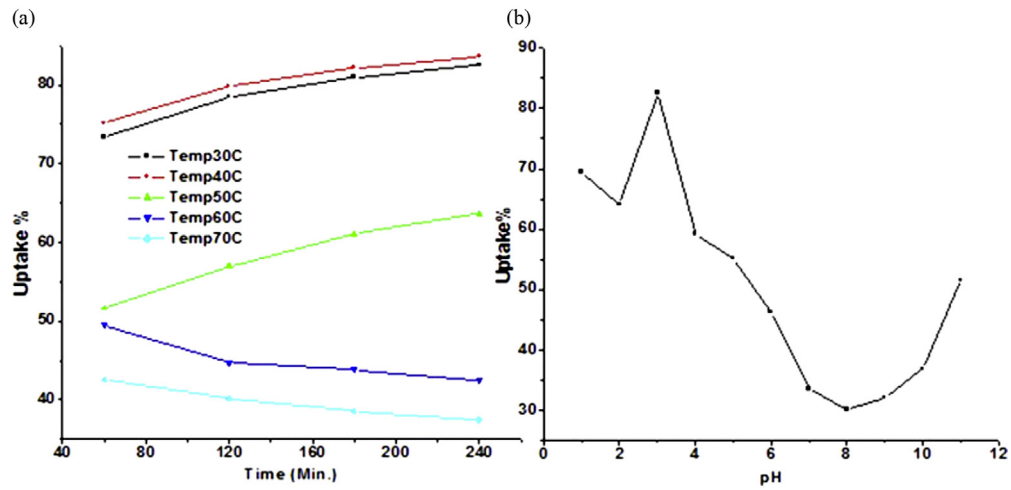

Fig. 7. (a) Effect of temperature and (b) pH variation.

There are two peaks in the N 1s spectrum of CH and CD at a BE of about 398.7 and 400.6 eV which could be attributed to the N atom in the R-NH_2 group and protonated R-NH_2. The N peaks at ~398 and 400 eV were slightly shifted to lower binding energies (0.1 and 0.7 eV, respectively) after adsorption of chromium suggesting the interaction between chromium and amino group to be predominantly non-specific electrostatic interaction. However, a peak of low intensity is observed at a BE ~401.6 eV which could be attributed to the formation of metal–NH_2 complex. The appearance of the N peak at higher binding energy is indicative of reduction in the electron cloud density of the nitrogen atom, probably due to the utilization of its lone pair in the formation of bond between N and Cr^{6+}. However, the low intensity of the peak suggests that the suggested bond formation could not be playing a major role in the uptake of Cr^{6+} by CD.

The O spectrum was deconvoluted into two peaks for CD loaded with Cr^{6+} while a single peak was present in C and CD. The peak at 532.2 eV can be attributed to C=O (acetate) in C and CD while in Cr^{6+}-loaded CD the peak at 531.8 eV can be attributed to carbonyl group and the peak at 533.1 eV can be attributed to the formation of $Cr(OH)_3$.

High-resolution spectra collected from the Cr 2p core region indicated that there was no Cr^{6+} on the adsorbent surface. However, it is evident from the spectra that there are two different species of Cr^{3+} present on the adsorbent with peaks at binding energies 576.9, 585.9, 579.0 and 588.5 eV. The positions of the peaks at 579.0 and 588.5 eV fall at the lower edge of the Cr^{6+} binding energies [36]. However, the spin orbit splitting values as well as FWHM values are quite low suggesting that the binding energies at 579.0 and 588.5 eV can also be attributed to Cr^{3+}. The XPS spectrum of oxygen indicates the presence of adsorbed water or hydroxyl groups (533.1 eV) and oxygen in carboxylate environment (531.8 eV). A peak for oxygen attributed to dichromate or chromate (~530 eV) could not be found [37]. This suggests that all of the chromium is present in +3 oxidation state in different forms, as $Cr(OH)_3$ and as Cr^{3+} stabilized by binding to carboxylate groups from DTPA. The high binding energies of 579 and 588.5 eV could be indicative of stabilization of Cr^{3+} by binding [38]. Therefore, it can be concluded that the Cr^{6+} was removed from aqueous phase and finally reduced to Cr^{3+}.

3.2. Adsorption–desorption studies

3.2.1. Effect of temperature

The uptake of chromium by CD was found to decrease with increase in temperature (Fig. 7a) representing the mechanism to be exothermic and that some desorption is happening at high temperatures [39].

3.2.2. Effect of pH

The adsorption capacity of CD for Cr^{6+} was found to be dependent on pH with maximum adsorption occurring at pH 3 (Fig. 7b) where the functional groups of CD are protonated favoring electrostatic attraction of Cr^{6+} and subsequent reduction to Cr^{3+}.

Volume = 25 ml, amount adsorbent = 0.05 g, $[Cr^{6+}]$ = 50 ppm (a) effect of temperature: pH = 3, contact time = 1–4 h, temp. = 30–70 °C. (b) pH variation: pH = 1–11, contact time = 4 h, temp. = 30 °C.

3.2.3. Sorption isotherm

The Cr^{6+} adsorption isotherms for CD were investigated and the isotherm constants for the models investigated are presented in Table 1. The fitting for all the isotherm models are presented in Fig. S3. The adsorption data for CD gave reasonably high correlation coefficient values for all the models studied. Fitting of Langmuir isotherm model suggested the presence of homogeneous adsorption sites. The well fit data of Freundlich model and the fact that Freundlich constant, n was greater than unity implied that the adsorption intensity was favorable over the entire range of concentrations studied. The fitting of Temkin model indicated favorable adsorption of Cr^{6+} while the high regression values for Halsey model suggested multilayer adsorption. The maximum adsorption capacity of CD for Cr^{6+} was found to be 192.3 mg/g. The comparison of maximum adsorption capacity of Cr^{6+} removal with other adsorbents available in literature are shown in Table 5 which indicates that CD has good adsorption potential for Cr^{6+} as compared to other adsorbents reported in literature.

3.2.4. Sorption kinetics

Kinetic models were studied and the fitting of all the models with experimental data are shown in Fig. S4 and the rate constants for the adsorption of Cr^{6+} by CD are presented in Table 2. The correlation coefficients for pseudo-second-order model were found to be greater than the other kinetic models for CD and the calculated equilibrium adsorption capacity values were closer to those obtained experimentally. This supported the assumption behind the model that the surface complexation may be the rate-limiting step involving valence forces through sharing or exchanging of electrons between adsorbent and adsorbate.

The plot of q_t versus $t^{1/2}$ did not pass through origin suggesting that intraparticle diffusion was not the only rate-controlling step

Table 5
Maximum Cr^{6+} sorption capacity (Q_{max}, mg/g) for various chitosan-based adsorbents reported in literature.

Adsorbent	Q_{max} (mg/g)	Reference
Quaternary chitosan salt	68.3	[2]
Chitosan cross-linked with epichlorohydrin	11.3	[39]
Chitosan bead	76.5	[56]
Chitosan on ceramic alumina	153.8	[57]
Magnetic chitosan	69.4	[57]
Chitosan/cellulose	13.05	[57]
Chitosan/perlite	153.8	[57]
Chitosan/montmorillonite	41.67	[57]
Non-crosslink chitosan	78	[58]
Raw chitosan	34.9	[59]
Chitosan/zeolite film	17.28	[60]
CACASC—chitosan-coated acid-treated *C. albidum* seed shells carbon	84.31	[61]
CCASC—chitosan-coated *C. albidum* seed shells carbon	76.23	[61]
Native chitosan	32.10	[62]
Crosslinked chitosan	28.2	[62]
Hydrolyzed crosslinked chitosan	24.50	[62]
Chitosan crosslinked with DTPA	192.3	In this study

but some degree of the boundary layer diffusion also controlled the adsorption process and that the overall rate of the metal adsorption process appeared to be controlled by more than one step. The reasonably good correlation coefficient for Bangham equation indicated that the diffusion of Cr^{6+} into the pores of the adsorbents under study also controlled the adsorption process. It was thus concluded that the metal adsorption process was controlled by more than one step.

3.2.5. Thermodynamic studies

The free energy change during the adsorption process was negative for low temperature and positive for higher temperatures for the experimental range of temperatures in Table 3 suggesting chemisorption to be the mechanism of adsorption. The negative value of enthalpy change indicated that the adsorption was physical in nature involving strong forces of attraction and is exothermic. The negative entropy change corresponded to decreasing in the degree of freedom of the adsorbed species.

3.2.6. Desorption

It is observed from Fig. 8 that maximum desorption (78.45%) happened in 0.1 N NaOH solution. This could be attributed to weakened electrostatic attraction between Cr^{3+} and CD due to the formation of $Cr(OH)_4^-$ on treatment with NaOH solution. Furthermore, it was also observed that chromium was not desorbed as Cr^{6+} (negligible color with diphenylcarbazide) but as Cr^{3+} affirming the fact that Cr^{6+} was almost completely converted into Cr^{3+} on CD. After desorption CD was reused up to three adsorption–desorption cycles and the results are presented in Fig. 8. It was found that the adsorption capacity of the CD decreased by 16% after the first cycle and ~10% the second cycle. Exposure of the adsorbent to alternate acidic and alkaline conditions during adsorption and desorption did not affect the stability of the adsorbent and its adsorption potential for chromium significantly.

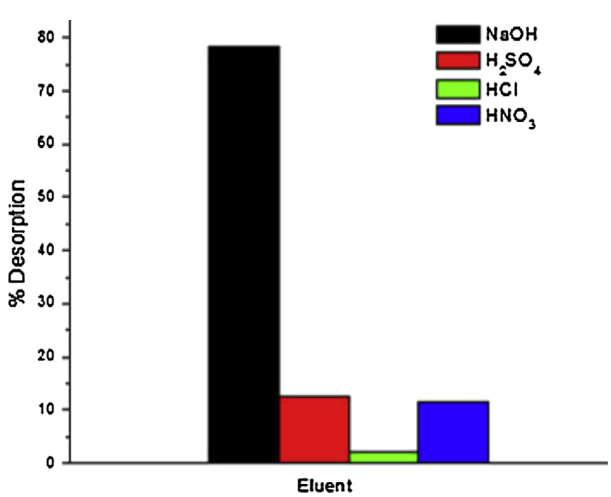

Fig. 8. Desorption study: contact time = 4 h, volume = 25 ml, amount of adsorbent = 0.05 g, temp. = 30 °C, [Cr^{6+}] = 500 ppm.

3.3. Application of adsorbent to chrome plating effluent

The results of the application of CD onto chrome plating effluent as an adsorbent with per cent extraction of major metals present in the effluent, their K_d values and selectivity coefficient of chromium over other metals are shown in Table 6. It is seen that CD is more effective adsorbent capable of removing more than 90% of Pb, Fe and Cr, >~50% Cu, Hg and Cd, ~10–20% Ni, Al, Zn and Mg. Selectivity coefficient was found to be highest for Cr over other metals present in the effluent for CD. Furthermore, the adsorbent also showed potential for the removal of Fe and Pb under the pH conditions optimal for removal of Cr^{6+} though their presence did not affect the removal of chromium in the concentration range present in the effluent. However, further investigations are warranted in this direction.

3.4. Environmental significance

In the present study, the use of CD resulted in complete reduction of Cr^{6+} to Cr^{3+} and the reduced Cr^{3+} remained adsorbed onto CD as Cr^{3+} could form a stable complex with DTPA unlike other adsorbents reported in literature where in the Cr^{6+} was only partly reduced to Cr^{3+} and the reduced Cr^{3+} was observed to leach into solution. Furthermore, CD was found to have potential for the treatment of chrome plating effluent which required minimum manipulation of pH.

3.5. Mechanism

The removal mechanism of Cr^{6+} from aqueous solution by non-living biomasses has been summarized by Park et al. [40] as three steps: (1) the binding of anionic Cr^{6+} ions with the positively charged groups on the biomass surface; (2) the reduction of Cr^{6+} to Cr^{3+} by adjacent electron-donor groups; (3) the release of Cr^{3+} ions into the aqueous phase due to electronic repulsion between the positively charged groups and the Cr^{3+} ions, or the formation of complexes of the Cr^{3+} with adjacent groups capable of Cr-binding. Furthermore, Park et al. [40] and Cerqueira et al. [41] have shown that the removal of Cr^{6+} is favored at lower pH as the reduction of Cr^{6+} to Cr^{3+} requires large quantities of protons and electrons in the reaction medium. After adsorption of Cr^{6+} on the adsorbent surface, the reduction of Cr^{6+} to Cr^{3+} is therefore initiated under acidic conditions, due to its high redox potential. Miretzky and Cirelli have identified that hydroxyl (—OH), carbonyl (C=O), and methoxy (O—CH_3) groups present on adsorbent surfaces can act as donors of electrons for the reduction reaction [42].

However, with most of the adsorbents only partial reduction of Cr^{6+} to Cr^{3+} has been reported and in some instances reduction of Cr^{6+} to Cr^{3+} in the aqueous phase.

The adsorption of chromium onto CD may have occurred in three steps: (1) the binding of anionic Cr^{6+} to protonated positively charged amino groups on the adsorbent surface, (2) the reduction of Cr^{6+} to Cr^{3+} by adjacent electron-donor groups and (3) the formation of clusters of Cr^{3+} on the adsorbent as indicated by ESR studies.

Table 6
Treatment of chrome plating effluent with CD.

Metals present in effluent	Initial concn. in the effluent (ppm)	% removal with CD	Distribution ratio, K_d	Selectivity coefficient for chromium
Cr	62.5	94.72	1184	–
Ni	14	17.85	223.2	5.3
Cu	10.1	21.78	272.3	4.35
Pb	4.4	100	1250	0.95
Hg	1.1	18.18	227.3	5.21
Al	15	14	175	6.77
Zn	236.2	13.76	171.96	6.89
Fe	232	96.29	1203.6	0.98
Mg	38.7	3.23	40.33	29.36
Cd	0.52	36.54	456.73	2.59

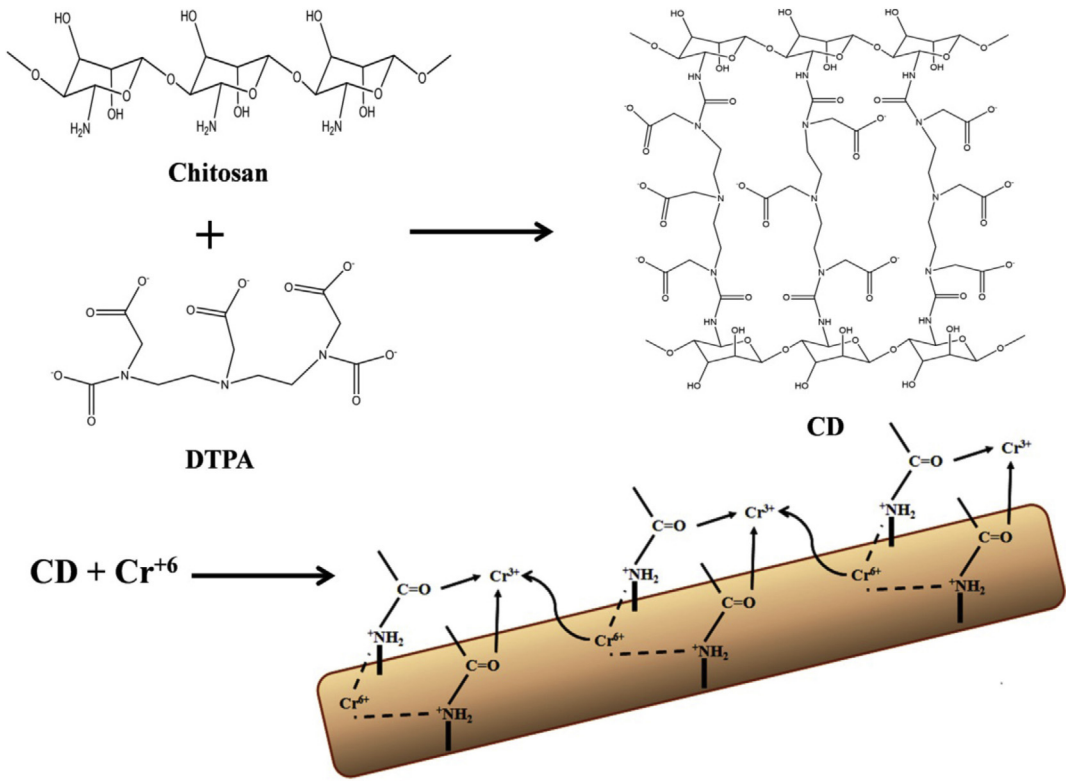

Scheme 1. Depiction of CD, adsorption of Cr^{6+} and its reduction to Cr^{3+} on the surface of CD.

Carboxyl and amino groups have been reported to be important in the reduction of Cr^{6+} to Cr^{3+} [43]. However, in contrast to the observations by Murphy et al., we did not observe any Cr^{3+} in solution. All of the adsorbed chromium was present as clusters of Cr^{3+}. The Cr^{3+} on the adsorbent surface may be bound with carbonyl (C=O) groups of DTPA through coordinate covalent bond (Scheme 1).

4. Conclusion

The potential of chitosan crosslinked with DTPA as adsorbent for Cr^{6+} was investigated. The optimum pH for removal of Cr^{6+} was found to be 3. Among the kinetic models tested, the adsorption kinetics was best described by the pseudo-second-order equation. The data fitted well with the Langmuir adsorption isotherm model. Adsorption thermodynamics indicate the adsorption of the metal onto CD to be exothermic process. XPS and ESR studies indicated the reduction of Cr^{6+} adsorbed onto CD to Cr^{3+}. The adsorbent could be successfully used for the removal of chromium from chrome plating effluents in the presence of several metal ions like Pb, Fe, Cu, Hg, Cd, Ni, Al, Zn and Mg. The adsorbent also showed potential for the removal of iron and lead.

Acknowledgement

The authors are thankful to Head, Department of Chemistry, for providing necessary facilities required to carry out this work. Ronak Bhatt is thankful to GNFC for giving support.

Appendix A. Supplementary data

Supplementary data associated with this article can be found, in the online version, at http://dx.doi.org/10.1016/j.ijbiomac.2014.12.041.

References

[1] G.N. Kousalya, M.R. Gandhi, S. Meenakshi, Int. J. Biol. Macromol. 47 (2010) 308–315.
[2] V.A. Spinelli, M.C.M. Laranjeira, V.T. Favere, React. Funct. Polym. 61 (2004) 347–352.
[3] S. Sugashini, S. Gopalakrishnan, Res. J. Chem. Sci. 2 (2012) 55–59.
[4] http://hppcb.gov.in/eiasorang/spec.pdf
[5] E. Repo, J.K. Warchol, T.A. Kurniawan, M.E.T. Sillanpaa, Chem. Eng. J. 161 (2010) 73–82.
[6] N. Li, R. Bai, C. Liu, Langmuir 21 (2005) 11780–11787.

[7] N.T.A. Ghani, G.A.E. Chaghaby, Int. J. Latest Res. Sci. Technol. 3 (2014) 24–42.
[8] W.S.W. Ngah, C.S. Endud, R. Mayanar, React. Funct. Polym. 50 (2002) 181–190.
[9] S. Quian, G. Huang, J. Jiang, F. He, Y. Wang, J. Appl. Polym. Sci. 77 (2000) 3216–3219.
[10] M. Dasha, F. Chiellini, R.M. Ottenbrite, E. Chiellini, Prog. Polym. Sci. 36 (2011) 981–1014.
[11] G.Z. Kyzas, M. Kostoglou, N.K. Lazaridis, Chem. Eng. J. 152 (2009) 440–448.
[12] S. Kushwaha, P.P. Sudhakar, Carbohydr. Polym. 86 (2011) 1055–1062.
[13] M.S. Alam, K. Inoue, K. Yoshizuka, H. Ishibashi, Sep. Sci. Technol. 33 (1998) 655–666.
[14] M. Rani, A. Agarwal, Y.S. Negi, J. Biomater. Nanobiotechnol. 2 (2011) 71–84.
[15] K. Oshita, A. Sabarudin, T. Takayanagi, M. Oshima, S. Motomizu, Talanta 79 (2009) 1031–1035.
[16] F. Zhao, E. Repo, D. Yin, M.E.T. Sillanpaa, J. Colloid Interface Sci. 409 (2013) 174–182.
[17] Y. Shimizu, S. Izumi, Y. Saito, H. Yamaoka, J. Appl. Polym. Sci. 92 (2004) 2758–2764.
[18] J. Roosen, K. Binnemans, J. Mater. Chem. A 2 (2014) 1530–1540.
[19] K. Inoue, K. Yoshizuka, K. Ohto, Anal. Chim. Acta 388 (1999) 209–218.
[20] E. Repo, R. Koivula, R. Harjula, M. Sillanpaa, Desalination 321 (2013) 93–102.
[21] E. Repo, J.K. Warchoł, A. Bhatnagar, M. Sillanpaa, J. Colloid Interface Sci. 358 (2011) 261–267.
[22] E. Repo, J.K. Warchoł, A. Bhatnagar, A. Mudhoo, M. Sillanpaa, Water Res. 47 (2013) 4812–4832.
[23] G.Z. Kyzas, N.K. Lazaridis, M. Kostoglou, J. Colloid Interface Sci. 407 (2013) 432–441.
[24] G.Z. Kyzas, M. Kostoglou, N.K. Lazaridis, D.N. Bikiaris, J. Hazard. Mater. 244–245 (2013) 29–38.
[25] G.Z. Kyzas, P.I. Siafaka, E.G. Pavlidou, K.J. Chrissafis, D.N. Bikiaris, Chem. Eng. J. 259 (2015) 438–448.
[26] A. Bobrowski, A. Krolicka, J. Zarebski, Electroanalysis 21 (2009) 1449–1458.
[27] S. Sander, T. Navratil, L. Novotny, Electroanalysis 15 (2003) 1513–1521.
[28] E. Repo, L. Malinen, R. Koivula, R. Harjula, M. Sillanpaa, J. Hazard. Mater. 187 (2011) 122–132.
[29] D.L. Rodman, N.A. Carrington, Z.L. Xue, Talanta 70 (2006) 668–675.
[30] S. Kalidhasan, A.S. KrishnaKumar, V. Rajesh, N. Rajesh, J. Colloid Interface Sci. 367 (2012) 398–408.
[31] C.K. Lin, J.N. Chen, C.C. Lin, J. Hazard. Mater. 56 (1997) 21–34.
[32] F. Ahmad, J. Alloys Compd. 586 (2014) 605–610.
[33] A. Nakajima, Y. Baba, Water Res. 38 (2004) 2859–2864.
[34] B.R. Araujo, J.O.M. Reis, E.I.P. Rezende, A.S. Mangrich, A. Wisniewski Jr., D.P. Dick, L.P.C. Romao, J. Environ. Manage. 129 (2013) 216–223.
[35] X. Qu, A. Wirsen, A-C. Albertsson, Polymer 41 (2000) 4589–4598.
[36] G.C. Allen, M.T. Curtis, A.J. Hooper, P.M. Tucker, J. Chem. Soc., Dalton Trans. 16 (1973) 1675–1683.
[37] M.C. Biesinger, C. Brown, J.R. Mycroft, R.D. Davidson, N.S. McIntyre, Surf. Interface Anal. 36 (2004) 1550–1563.
[38] E. Groppo, C. Lamberti, S. Bordiga, G. Spoto, A. Zecchina, Chem. Rev. 105 (2005) 115–184.
[39] S. Pandey, S.B. Mishra, J. Colloid Interface Sci. 361 (2011) 509–520.
[40] D. Park, Y.S. Yun, J.M. Park, Environ. Sci. Technol. 38 (2004) 4860–4864.
[41] S.C.A. Cerqueira, L.P.C. Romao, S.C.O. Lucas, L.E. Fraga, M.L. Simoes, P. Hammer, J.R. Lead, A.P. Mangoni, A.S. Mangrich, Fuel 91 (2012) 141–146.
[42] P. Miretzky, A.F. Cirelli, J. Hazard. Mater. 180 (2010) 1–19.
[43] V. Murphy, H. Hughes, P. McLoughlin, Chemosphere 70 (2008) 1128–1134.
[44] H.M.F. Freundlich, J. Phys. Chem. 57A (1906) 385–470.
[45] S. Schiewer, S.B. Patil, Bioresour. Technol. 99 (2008) 1896–1903.
[46] S.Y. Elovich, O.G. Larinov, Russ. Chem. Bull. 11 (1962) 198–203.
[47] M.J. Temkin, V. Pyzhev, Acta Physiochim. USSR 12 (1940) 217–222.
[48] C. Theivarasu, S.E. Mylsamy, J. Chem. 8 (2011) 363–371.
[49] G. Halsey, J. Chem. Phys. 16 (1948) 931–937.
[50] S. Lagergren, K. Sven, Vetenskapsakad. Handl. Band 24 (1898) 1–39.
[51] Y.S. Ho, Adsorption of Heavy Metals from Waste Streams by Peat, PhD thesis, University of Birmingham, Birmingham, UK (1995).
[52] A. Ornek, M. Ozacar, I.A. Sengil, Biochem. Eng. J. 37 (2007) 192–200.
[53] W.J. Weber, J.C. Morris, J. Sanit. Eng. Div. Am. Soc. Civ. 89 (1963) 31–60.
[54] R.K. Rajoriya, B. Prasad, I.M. Mishra, K.L. Wasewar, Chem. Biochem. Eng. Q. 21 (2007) 219–226.
[55] G.E. Boyd, A.W. Adamson, L.S. Myers Jr., J. Am. Chem. Soc. 69 (1947) 2836–2848.
[56] S. Bosinco, E. Guibal, J. Roussy, P. Lecloirec, Miner. Process. Extr. Metall. Rev. 19 (1998) 277–291.
[57] W.S. Wan Ngah, L.C. Teong, M.A.K.M. Hanafiah, Carbohydr. Polym. 83 (2011) 1446–1456.
[58] R. Schmuhl, H.M. Krieg, K. Keizer, Water SA 27 (2001) 1–8.
[59] P. Udaybhaskar, L. Iyengar, A.V.S. Prabhakara Rao, J. Appl. Polym. Sci. 39 (1990) 739–747.
[60] A.C.L. Batista, E.R. Villanueva, R.V.S. Amorim, M.T. Tavares, G.M. Campos-Takaki, Molecules 16 (2011) 3569–3579.
[61] O.S. Amuda, F.E. Adelowo, M.O. Ologunde, Colloid. Surf. B 68 (2009) 184–192.
[62] S.P. Ramnani, S. Sabharwal, React. Funct. Polym. 66 (2006) 902–909.